AD

AD-E402 938

Technical Report ARWEC-TR-01007

A METHOD FOR PREDICTING FRAGMENTATION CHARACTERISTICS OF NATURAL AND PREFORMED EXPLOSIVE FRAGMENTATION MUNITIONS

Vladimir M. Gold
Ernest L. Baker
Koon W. Ng
John M. Hirlinger

September 2001

US ARMY
TANK AUTOMOTIVE AND
ARMAMENTS COMMAND
ARMAMENT RDE CENTER

U.S. ARMY ARMAMENT RESEARCH, DEVELOPMENT AND ENGINEERING CENTER

Warheads, Energetics & Combat-support Armament Center

Picatinny Arsenal, New Jersey

REPORT DOCUMENTATION PAGE

Form Approved
OMB No. 0704-01-0188

PLEASE DO NOT RETURN YOUR FORM TO THE ABOVE ADDRESS.

1. REPORT DATE *(DD-MM-YYYY)*	2. REPORT TYPE	3. DATES COVERED *(From - To)*
September 2001	Final	

4. TITLE AND SUBTITLE

A METHOD FOR PREDICTING FRAGMENTATION CHARACTERISTICS OF NATURAL AND PREFORMED EXPLOSIVE FRAGMENTATION MUNITIONS

5a. CONTRACT NUMBER

5b. GRANT NUMBER

5c. PROGRAM ELEMENT NUMBER

6. AUTHORS

Vladimir M. Gold, Ernest L. Baker, Koon W. Ng, and John M. Hirlinger

5d. PROJECT NUMBER

5e. TASK NUMBER

5f. WORK UNIT NUMBER

7. PERFORMING ORGANIZATION NAME(S) AND ADDRESS(ES)

ARDEC, WECAC
Energetics & Warheads Division (AMSTA-AR-WEE-C)
Picatinny Arsenal, NJ 07806-5000

8. PERFORMING ORGANIZATION REPORT NUMBER

9. SPONSORING/MONITORING AGENCY NAME(S) AND ADDRESS(ES)

ARDEC, WECAC
Information Research Center (AMSTA-AR-WEL-T)
Picatinny Arsenal, NJ 07806-5000

10. SPONSOR/MONITOR'S ACRONYM(S)

11. SPONSOR/MONITOR'S REPORT NUMBER(S)

Technical Report ARWEC-TR-01007

12. DISTRIBUTION/AVAILABILITY STATEMENT

Approved for public release; distribution is unlimited.

13. SUPPLEMENTARY NOTES

14. ABSTRACT

New methodology for simulating performance of explosive fragmentation munitions presented in this work integrates three-dimensional axisymmetric hydrocode analyses with analytical fragmentation modeling. The newly developed computational technique is applied to both the natural and preformed explosive fragmentation munitions problems. The developed model remarkably accurately predicts the fragment spray experimental data.

15. SUBJECT TERMS

Fragmentation, Fracture, Fracture modeling, Numerical modeling

16. SECURITY CLASSIFICATION OF:			17. LIMITATION OF ABSTRACT	18. NUMBER OF PAGES	19a. NAME OF RESPONSIBLE PERSON
a. REPORT	b. ABSTRACT	c. THIS PAGE			19B. TELEPHONE NUMBER *(Include area code)*
UNCLASSIFIED	UNCLASSIFIED	UNCLASSIFIED	SAR	22	

CONTENTS

	Page
CALE Model	1
The Natural Fragmentation Model	1
The Natural Fragmentation Analyses: the Results	4
Preformed Fragmentation Modeling	5
Summary	5
References	17
Distribution List	19

FIGURES

1	Results of CALE-code modeling: initial configuration and CALE's predictions following the explosive detonation initiation	7
2	Natural fragmentation model schematic	8
3	Fragment mass distribution versus spray angle Θ for varying fragmentation times	9
4	Fragment velocity distribution versus spray angle Θ	10
5	Cumulative number of fragments in the fragment spray versus the fragment size m/μ	11
6	Number of fragments in the fragment spray: varying the shell fragmentation time and the γ	12
7	Number of fragments with mass greater than 3 grains versus spray angle Θ	13
8	Fragment velocity distribution versus spray angle Θ for a spherical-shell charge	14
9	Number of fragments versus spray angle Θ for a spherical-shell charge with preformed 3-grain fragments	15

CALE MODEL

Numerical simulations presented in this work were performed using the CALE computer program (ref. 1). CALE is a two-dimensional and three-dimensional axial symmetric high rate finite difference computer program based on arbitrary Lagrangian-Eulerian formulation of the governing equations.

The geometry of two problems under the consideration is shown in figure 1. As shown in the figure, upon initiation of the high explosive charge, rapid expansion of high-pressure high-velocity detonation products results in high-strain high-strain-rate dilation of the hardened steel shell, accompanied by the implosion of the copper shaped charge liner that produces a high-speed metal jet moving along the charge's axis of symmetry z.

In addition to specification of the problem geometry and initial and boundary conditions, equations of states and constitutive equations for all materials have to be specified before the solution procedure can be initiated. The explosive was modeled using the Jones-Wilkins-Lee-Baker equation of state employing a set of parameters (ref. 2) resulting from thermo-chemical equilibrium analyses of detonation products with the JAGUAR code. The hydrodynamic responses of the steel shell and the copper liner were modeled using a standard linear polynomial approximation usually employed for metals. The constitutive behavior of these metals was modeled using the Steinberg-Guinan yield-strength model and the von Mises yielding criterion. A standard set of parameters available from Tipton (ref. 3) was employed in the analyses.

Since the extent of dilation of the rapidly expanding steel shell is limited by its strength, at some point the shell ruptures generating a spray of steel fragments moving with trajectories at angles Θ with z-axis. Accordingly, the principal topic of this work will be a numerical model for analytical description of parameters of this spray as functions of the spray angle Θ. In typical explosive fragmentation tests (arena tests), the tested munitions are positioned at the origin of the reference polar coordinate system, and surrounded with series of velocity-measuring screens and fragment-catching witness panels, all at significant distances from the warhead. Accordingly, the fragmentation characteristics are assessed as functions of polar angles Θ' identifying angular positions of these measuring devices. Assuming that the fragment trajectory angles Θ do not change with time (that is the lateral drift of fragments due to air resistance is small) and that definitions of angles Θ and Θ' are approximately identical, the developed model enables prediction of crucial characteristics of explosive fragmenting munitions including the number of fragments, the fragment size distribution, and the average fragment velocities.

THE NATURAL FRAGMENTATION MODEL

The developed natural fragmentation model is based on the Mott's theory of break-up of cylindrical "ring-bombs" (ref. 4), in which the average length of the resulting circumferential fragments is a function of the radius and velocity of the ring at the moment of break-up, and the mechanical properties of the metal. Following Mott and Linfoot (ref. 5), the "random variations" in fragment sizes are accounted through the following fragment distribution relationship

$$N(m) = N_0 e^{-\left(m/\mu\right)^{1/2}} \tag{1}$$

In equation 1, $N(m)$ represents total number of fragments of mass greater than m, μ is defined as one half of the average fragment mass, $N_0 = M/\mu$, and M is the total mass.

In attempting to evaluate the distribution of fragment sizes occurring in the dynamic fragmentation of expanding metal rings, Mott (ref. 4) introduced an idealized model in which the average circumferential fragment lengths are not random but determined by the interaction of stress release waves originating from instantaneous fractures in the body. A schematic of the Mott's model is shown in figure 2a. Assuming that a fracture in the ring is supposed to have occurred first at A_1 and that stress release waves have traveled to points B_1 and $\underline{B}_1$, further fractures can no longer take place in regions A_1B_1 and $\underline{A}_1\underline{B}_1$. On the other hand, in the regions B_1B_2 and $\underline{B}_1\underline{B}_2$ the plastic strain is increasing, which increases the probability of fractures at any point in these regions, especially at points B_1, B_2, $\underline{B}_1$, and $\underline{B}_2$. Thus, according to Mott's theory the average size of fragments is determined by the rate at which stress relieved regions A_1B_1 and $\underline{A}_1\underline{B}_1$ spread through the plastically expanding ring.

At the moment of fracture, let r be the radius of the ring and V be the velocity with which the shell is moving outwards. Then, according to Mott (ref, 4), the average circumferential length of the resulting fragments is

$$x_0 = \left(\frac{2P_F}{\rho\gamma}\right)^{1/2} \frac{r}{V} \tag{2}$$

In equation 2, ρ and P_F denote the density and the strength, respectively; and γ is a semi-empirical statistical constant determining the dynamic fracture properties of the material.

Given that the shape and the average fragment lengths are know, the idealized averaged fragment mass can be calculated. For example, assuming approximately cubic-shaped fragments, μ takes the following form

$$\mu = \frac{1}{2}\rho x_0^3 \tag{3}$$

A schematic for the newly developed technique integrating CALE-code analyses with Mott's fragmentation model is shown in figure 2b. The details of this technique are as follows. For computational purposes, the shell is discretized into a finite number of short "ring" segments, N. For each discrete ring element j, uniform field variables are assumed. Accordingly, the masses, the velocities and radii of ring segments j are defined by the mass averages of the respective parameters:

$$m_j = \sum_{L_j} m_i \tag{4}$$

$$v_j = \frac{\sum_{L_j} v_i m_i}{m_j} \tag{5}$$

$$r_j = \frac{\sum_{L_j} R_i m_i}{m_j} \cdot \frac{1}{\sin \Theta_j} \tag{6}$$

$$\Theta_j - \frac{\pi}{2N} \le \Theta_i < \Theta_j + \frac{\pi}{2N} \tag{7}$$

In equations 4 through 6, m_i, v_i, and R_i denote the mass, the velocity, and the radial coordinate of the $i-th$ computational cell from the CALE-code generated data. L_j denotes a number of computational cells contained in the $j-th$ ring segment. Θ_j denotes the Θ –angle that corresponds to the $j-th$ ring segment given by

$$\Theta_j = \frac{\pi}{2N} \cdot \left(j - \frac{1}{2} \right) \tag{8}$$

For each computational cell i, the velocity v_i and the Θ –angle Θ_i are calculated respectively by

$$v_i = \sqrt{v_{zi}^2 + v_{Ri}^2} \tag{9}$$

and

$$\Theta_i = \arctan \frac{v_{Ri}}{v_{zi}} \tag{10}$$

In equations 9 and 10, v_{zi} and v_{Ri} denote the axial and the radial velocity components from the CALE-code generated data.

Given that the velocities and the radii of ring segments j are determined through equations 5 and 6, the resulting fragment size distributions can be calculated through the following relationships

$$N_j(m) = N_{0j} e^{-\left(m/\mu_j\right)^{1/2}} \tag{11}$$

$$\mu_j = \sqrt{\frac{2}{\rho}} \left(\frac{P_F}{\gamma} \right)^{3/2} \left(\frac{r_j}{V_j} \right)^3 \tag{12}$$

$$N_{0j} = \frac{m_j}{\mu_j} \tag{13}$$

THE NATURAL FRAGMENTATION ANALYSES: THE RESULTS

The fundamental assumption of all fragmentation analyses presented in this work was that the fragmentation occurs instantly throughout the entire body of the shell. Following Mott's critical fracture strain concept (ref. 4) and assuming that for given shell geometry and materials, the shell fragmentation time is a function of the cumulative dilatational plastic strain in the shell, the shell fragmentation time can be conveniently expressed in terms of the global shell dilatational properties. Given that in a typical fragmentation munition device the explosive is tightly confined inside the shell, the cumulative strains of the expanding explosive and the surrounding shell are nearly proportional. Accordingly, the critical fracture strain at the moment of the shell break-up may be conveniently measured in terms of the high explosive detonation products volume expansions, V/V_0. The developed technique had been validated employing experimental data from the cylindrical-shell charge shown in figure 1a. As shown in figures 3 through 7, this relatively simplistic model remarkably accurately predicts the fragment spray experimental data.

Figures 3 and 4 show the effect of the shell fragmentation time on the fragment spray mass and velocity distribution functions. The seemingly significant disagreement between the experimental velocities and the analyses for $\Theta \leq 15$ deg is due to deliberate omission of the shaped charge jet data from the fragmentation analyses; mainly because of the minimal contribution to the fragment-spray lethality. Accordingly, the copper shaped charge jet had been neglected in all fragmentation analyses, although included in the CALE model in order to maintain proper explosive confinement parameters. As shown in figures 3 and 4, varying the shell fragmentation time from approximately 5 μs (at which the detonation products had expanded approximately 1.8 times its original volume, $V/V_0 \approx 1.8$) to approximately 30 μs ($V/V_0 \approx 31.9$), the changes in the fragment spray angles Θ were rather small, while the fragment spray velocities were affected rather significantly. As shown in figure 4, delaying the moment of the shell break-up had resulted in considerable increases of the fragment spray velocities, apparently due to the prolonged "pressurized" interaction with expanding detonation products that increased the total momentum transferred to the shell.

As shown in figures 3 and 4, the analyses reasonably accurately reproduce overall shapes of the fragment spray mass and velocity distribution curves, including the principal (that is the maximum lethality) peak at $\Theta \approx 90$ deg. The disagreement between the analyses and the 45-deg and the 60-deg fragment spray mass spikes is due to fragments from the shaped charge liner-retaining ring, which had not been included in the CALE model, mainly because of the minimal effect on the overall fragment lethality.

Figures 5 and 6 show plots of the number of fragments in the fragment spray as functions of the fragment size m/μ, the spray angle Θ, the shell fragmentation time, and the dynamic fracture parameter γ. As shown in the figures, increases in the parameter γ had resulted in increases of the number of fragments N, both for the $N - m/\mu$ and the $N - \Theta$ relationships. These results are in agreement with the Mott's theory (ref. 4), according to which the parameter γ defines the probability of fracture in the plastically expanding shell determining the number of breaks in the circumferential direction.

As shown in figure 5, a series of values of the parameter γ were obtained by fitting the analytical fragment size distribution functions, equation 11, with the experimental data, all analyses repeated for each assumed shell fragmentation time. As shown in the figure, nearly identical fragment distribution curves had resulted from both the 8 μs ($V/V_0 \approx 3.0$) and the 20 μs ($V/V_0 \approx 14.1$) fragmentation times. The accepted shell fragmentation time was determined from the high-speed photographic data of Pearson (ref. 6). Following Pearson (ref. 6), the fragmentation of shells with cylindrical geometries (similar to that considered in this work) occurs approximately at three volume expansions, the fragmentation being defined as the instant at which the detonation products first appear as they emanate from the fractures in the shell. Accordingly, the accepted shell fragmentation was approximately 8 μs ($V/V_0 \approx 3.0$) and the value of γ = 12 was selected for all further analyses.

Figure 7 shows a plot of the number of fragments with mass greater than 3 grains versus the spray angle Θ, which is a principal lethality parameter of the fragment spray of the munition. The disagreement between the analyses and small spikes at 45 deg and 60 deg is due to fragments from the shaped charge liner-retaining ring, which had not been included in the CALE model, mainly because of the minimal effect on the overall fragment lethality. The disagreement between the analyses and the spike at 155 deg is due to fragments from a rotating band that had not been included in the CALE model. As shown in the figure, given a relatively crude assumption of the shell fragmentation time, the overall agreement between the analyses and the experimental data is rather remarkable.

PREFORMED FRAGMENTATION MODELING

Figures 8 and 9 show plots of fragment velocities and number of fragments versus the spray angle Θ for a preformed fragment spray generated by the spherical-shell explosive charge shown in figure 1b. As shown in figure 8, the spherical-shell charge produces approximately uniform fragment spray with fragment velocities increasing with the delayed shell break-up time. Figure 9 shows a plot of number of fragments with approximately 3-grain fragment sizes versus the spray angle Θ. Assuming an ideally uniform fragment size distribution, the number of fragments in the preformed–fragment spray is

$$N_j = \frac{m_j}{2\mu_0} \tag{14}$$

where μ_0 is one half of the mass of the preformed fragment and m_j is the mass of the $j-th$ ring segment.

SUMMARY

New methodology for simulating performance of explosive fragmentation munitions presented in this work integrates three-dimensional axisymmetric hydrocode analyses with analytical fragmentation modeling. The newly developed computational technique is applied to both the natural and preformed explosive fragmentation munitions problems. The developed model remarkably accurately predicts the fragment spray experimental data.

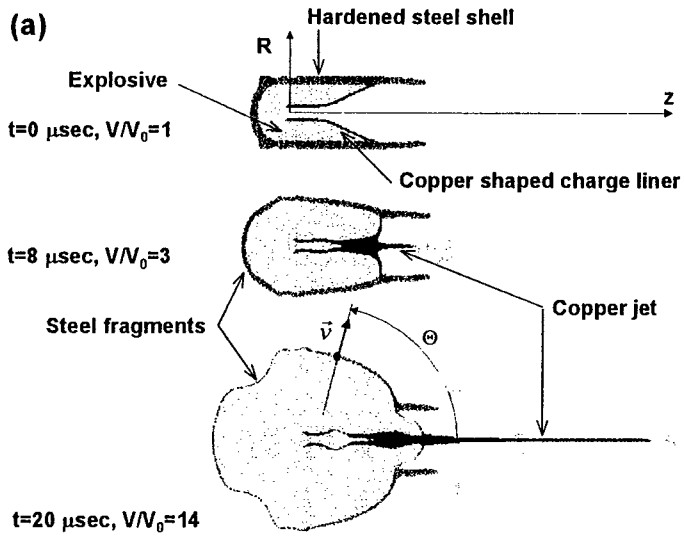

(a)
Cylindrical shell charge

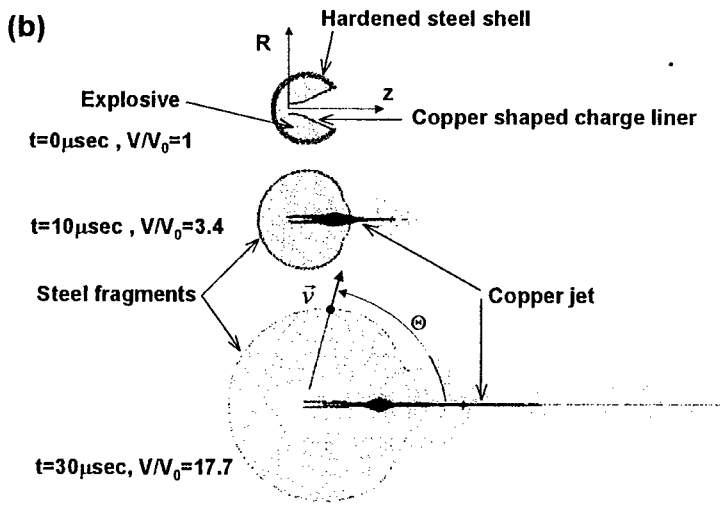

(b)
Spherical shell charge

Figure 1
Results of CALE-code modeling: initial configuration and CALE's predictions following the explosive detonation initiation

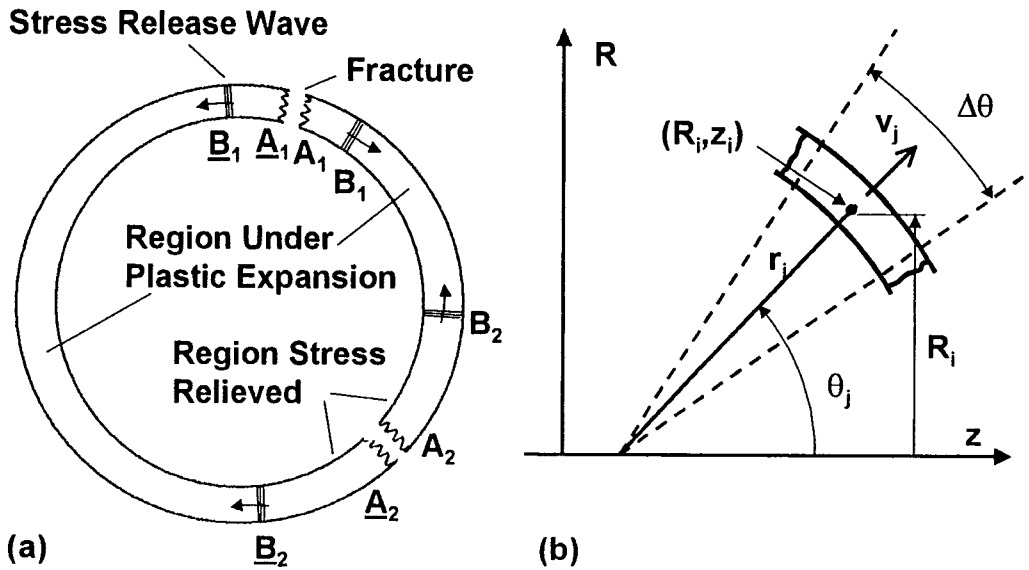

Figure 2
Natural fragmentation model schematic

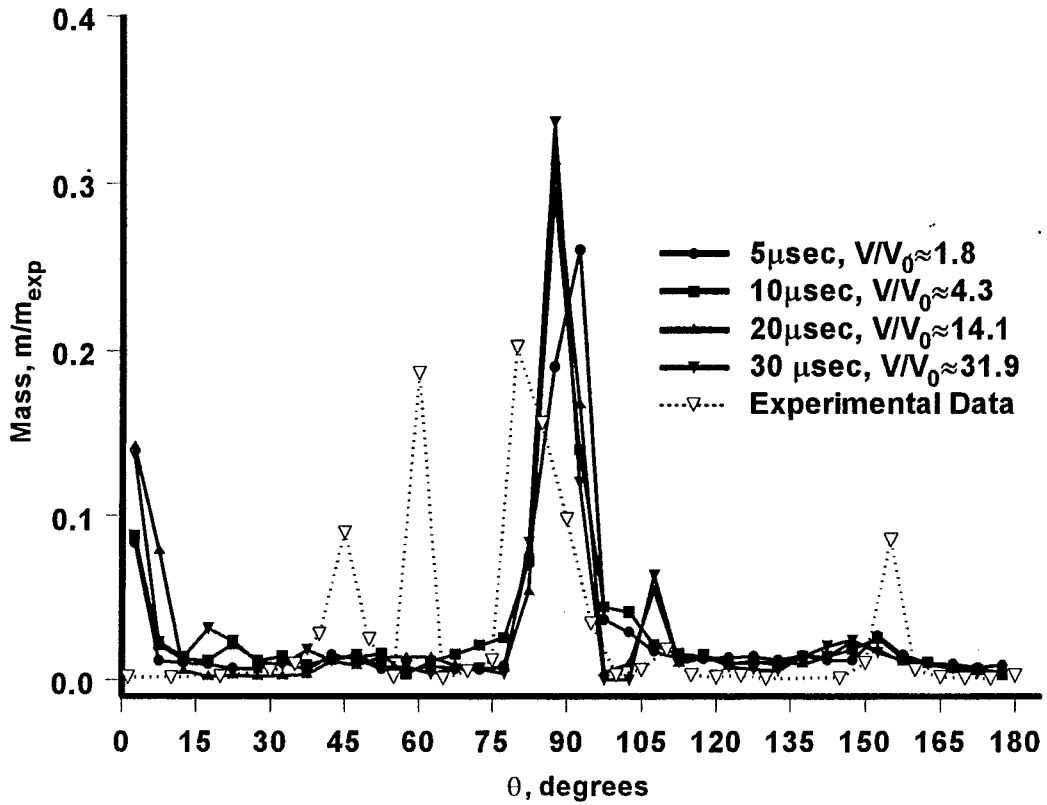

Figure 3
Fragment mass distribution versus spray angle Θ for varying fragmentation times

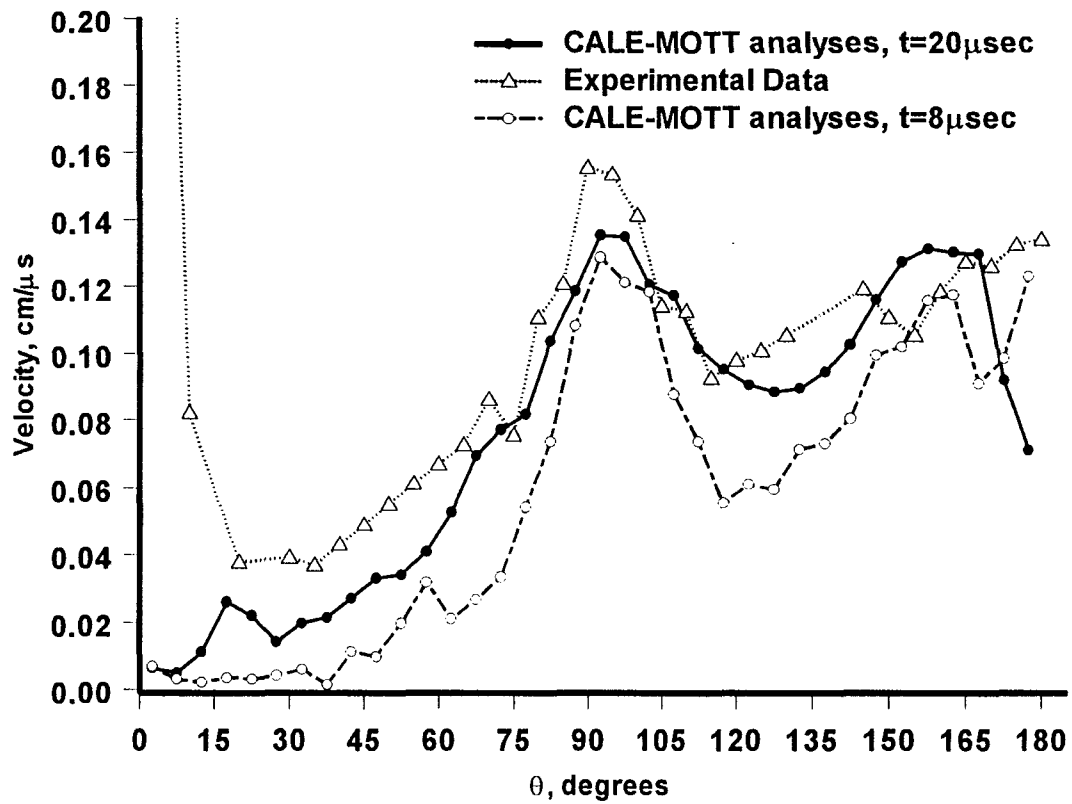

Figure 4
Fragment velocity distribution versus spray angle Θ

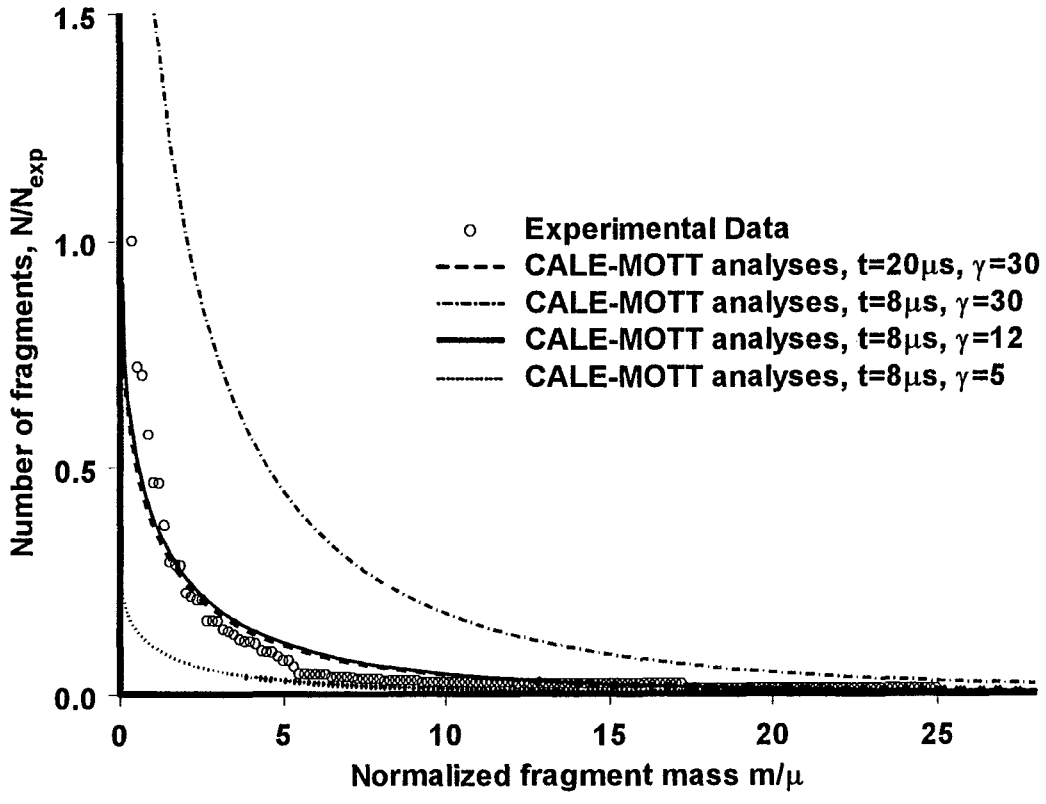

Figure 5
Cumulative number of fragments in the fragment spray versus the fragment size m/μ

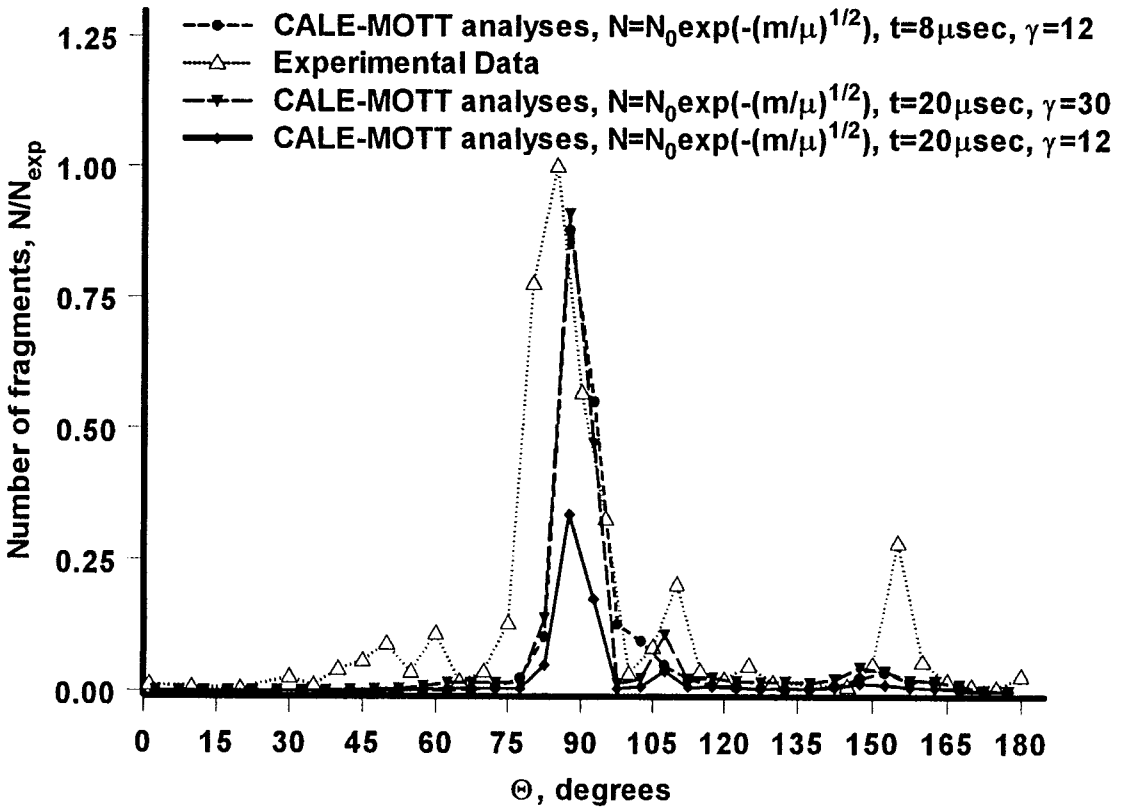

Figure 6
Number of fragments in the fragment spray: varying the shell fragmentation time and the γ

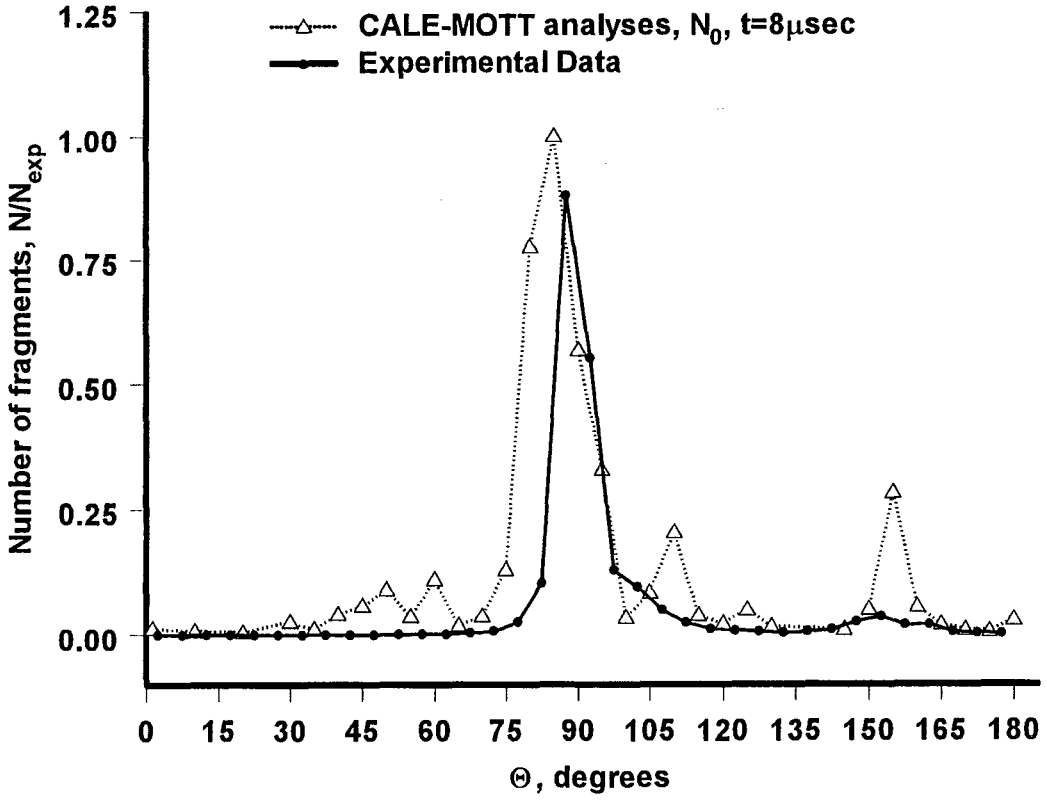

Figure 7
Number of fragments with mass greater then 3 grains versus spray angle Θ

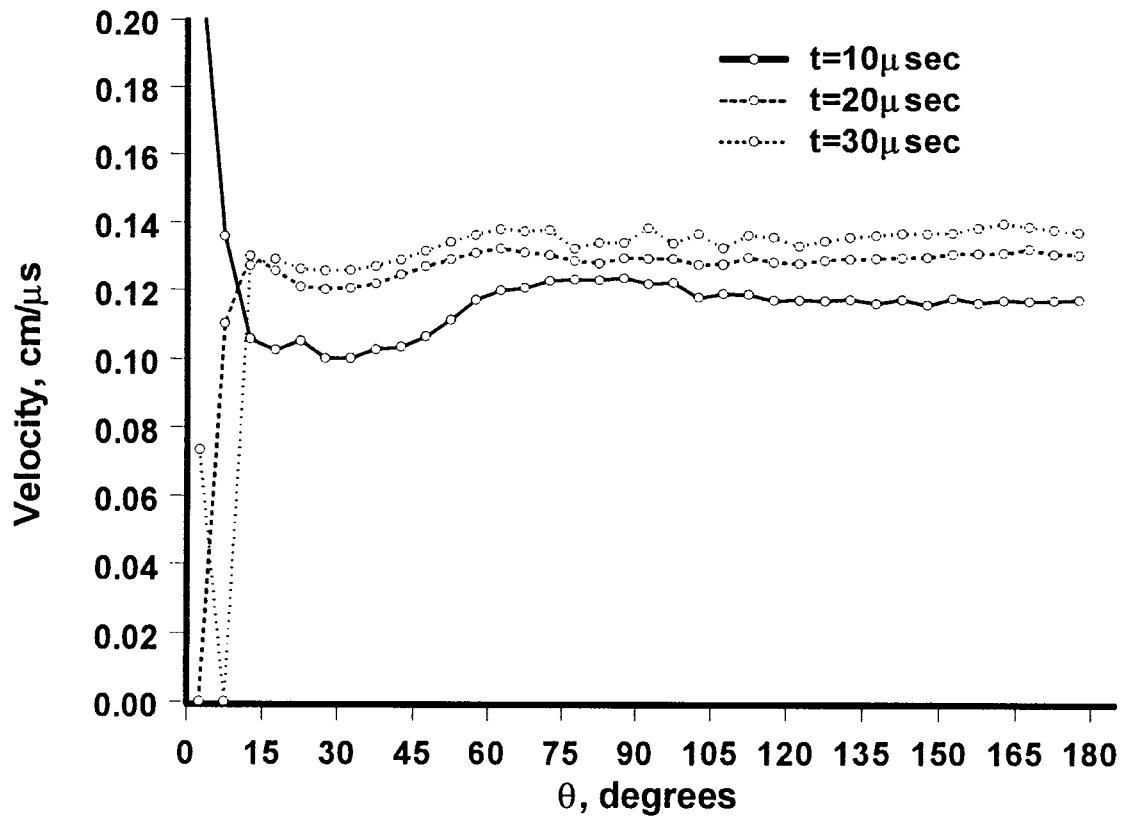

Figure 8
Fragment velocity distribution versus spray angle Θ for a spherical-shell charge

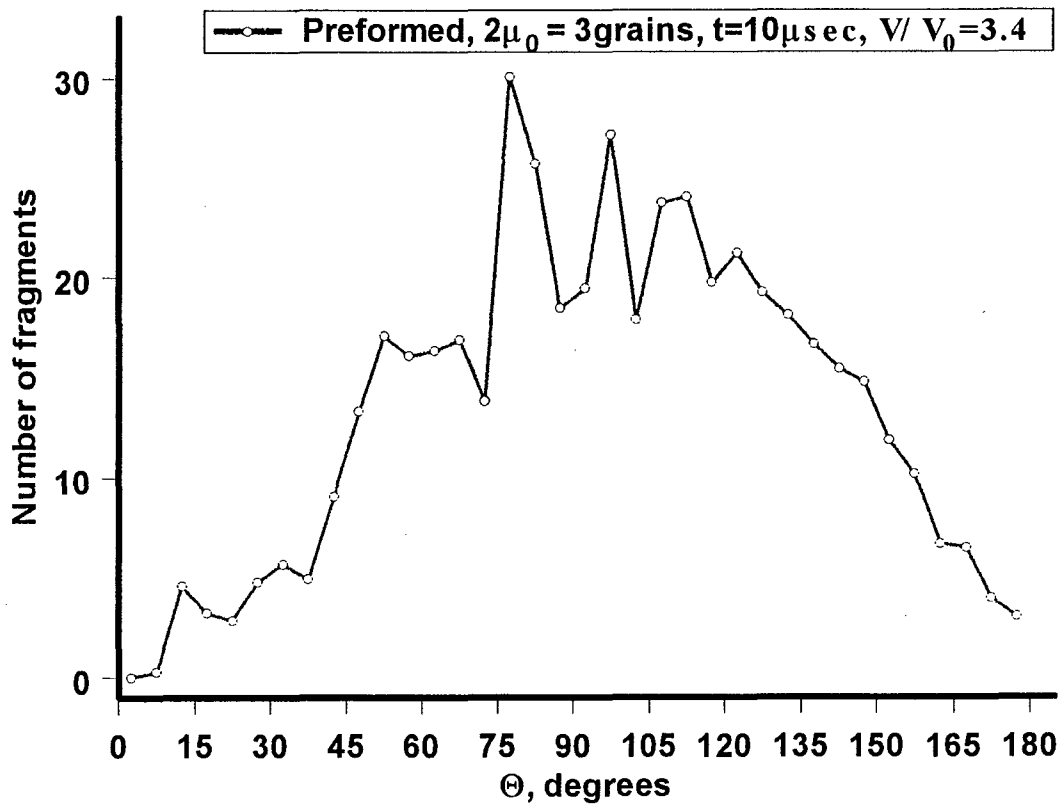

Figure 9
Number fragments versus spray angle Θ for a spherical shell charge with preformed 3-grain fragments

REFERENCES

1. Tipton, R. E., "CALE Users Manual," Version 910201, Lawrence Livermore National Laboratory, 1991.

2. Baker, E. L., Private communications, 2000.

3. Tipton, R. E., "EOS Coefficients for the CALE Code for Some Materials," Lawrence Livermore National Laboratory, 1991.

4. Mott, N. F., F.R.S., "Fragmentation of Steel Cases," Proc. Roy. Soc., 189, pp. 300-308, 1947.

5. Mott, N. F. and Linfoot, E. H., "A Theory of Fragmentation," Ministry of Supply, A.C. 3348, January 1943.

6. Pearson, J., "A Fragmentation Model for Cylindrical Warheads", Technical Report NWC TP 7124, Naval Weapons Center, China Lake, California, December 1990.

DISTRIBUTION LIST

Commander
Armament Research, Development and Engineering Center
U.S. Army Tank-automotive and Armaments Command
ATTN: AMSTA-AR-WEL-T (2)
AMSTA-AR-GCL
AMSTA-AR-WEE-C, E. Baker
V. Gold (5)
K. Ng
AMSTA-AR-CCL-C, J. Hirlinger
G. Fleming
AMSTA-AR-CCL-D, S. Liss
G. Moshier
AMSTA-AR-WEA, G. Voorhis
Picatinny Arsenal, NJ 07806-5000

Defense Technical Information Center (DTIC)
ATTN: Accession Division
8725 John J. Kingman Road, Suite 0944
Fort Belvoir, VA 22060-6218

Director
U.S. Army Materiel Systems Analysis Activity
ATTN: AMXSY-EI
392 Hopkins Road
Aberdeen Proving Ground, MD 21010-5423

Commander
Chemical/Biological Defense Agency
U.S. Army Armament, Munitions and Chemical Command
ATTN: AMSCB-CII, Library
Aberdeen Proving Ground, MD 21010-5423

Director
U.S. Army Edgewood Research, Development and Engineering Center
ATTN: SCVRD-RTB (Aerodynamics Technology Team)
Aberdeen Proving Ground, MD 21010-5423

Director
U.S. Army Research Laboratory
ATTN: AMSRL-OP-CI-B, Technical Library
Aberdeen Proving Ground, MD 21005-5066

Chief
Benet Weapons Laboratory, CCAC
Armament Research, Development and Engineering Center
U.S. Army Tank-automotive and Armaments Command
ATTN: AMSTA-AR-CCB-TL
Watervliet, NY 12189-5000

Director
U.S. Army TRADOC Analysis Command - WSMR
ATTN: ATRC-WSS-R
White Sands Missile Range, NM 88002

Commander
Naval Air Warfare Center Weapons Division
1 Administration Circle
ATTN: Code 473C1D, Carolyn Dettling (2)
China Lake, CA 93555-6001

GIDEP Operations Center
P.O. Box 8000
Corona, VA 91718-8000

Alliant Tech Systems
ATTN: C. Nelson
G. Holms
600 Second Street NE
Hopkins, MN 55343

The views, opinions, and/or findings contained in this report are those of the author(s) and should not be construed as an official Department of the Army position, policy, or decision, unless so designated by other documentation.

The citation in this report of the names of commercial firms or commercially available products or services does not constitute official endorsement by or approval of the U.S. Government.

Destroy this report when no longer needed by any method that will prevent disclosure of its contents or reconstruction of the document. Do not return to the originator.